Int. J. Electrochem. Sci., 17 **(2022)** Article Number: 221126, doi: 10.20964/2022.11.29

International Journal of
ELECTROCHEMICAL
SCIENCE
www.electrochemsci.org

Determination of Digoxin glycoside in foxglove flower using Ag_2S/CNTs nanocomposites

Yuhui He[1], *Yi Zheng*[2,*]

[1] School of Architecture and Urban Planning, Changchun University of Architecture and Civil Engineering, Changchun, Jilin, 130000, China
[2] Changchun Sci Tech Univ, Sch Life Sci, Changchun, Jilin, 130000, China
[*]E-mail: zhengyick495081@sina.com

Received: 4 August 2022 / *Accepted:* 8 September 2022 / *Published:* 10 October 2022

The current study's objective was to create a nanocomposite of Ag_2S/CNTs by electrodepositing them on the surface of a glassy carbon electrode (GCE), which would then serve as a sensitive and focused electrochemical sensor to quantify the amount of digoxin in a prepared genuine sample of foxglove. According to structural investigations performed using FE-SEM and XRD, an Ag_2S/CNTs nanocomposite was successfully electrodeposited on the GCE surface. Ag_2S/CNTs/GCE as a sensitive and selective Digoxin sensor demonstrated a quick reaction time, a steady electrocatalytic response, and a linear relationship to the concentration of Digoxin from 0 to 24ng/mL according to electrochemical tests employing CV, DPV, and amperometry. The sensitivity was 0.31287μA/ng.mL^{-1}, and the detection limit was 0.001ng/mL. The accuracy of Ag_2S/CNTs/GCE was tested for the purpose of determining Digoxin in genuine samples of foxglove flowers that had been prepared. The findings exhibited acceptable RSD levels and demonstrated good agreement between the results of both analyses for further samples (3.47% to 4.41%). These results showed that the suggested procedure has been successfully used to determine digoxin in floral extract.

Keywords: Hierarchical nanostructure; Nanocomposite; Ag_2S nanoparticles; CNTs; Digoxin; Glycoside, Foxglove Flower; Amperometry

1. INTRODUCTION

Glucose, a sugar that is linked to another functional group by a glycosidic bond, is the source of glycoside. In living things, glycosides perform a variety of critical functions [1, 2]. Inactive glycosides are the primary form of chemical storage in many plants [3, 4]. Steviol glycosides are used in a variety of ways, including as a substitute for sugar in food, as a component of medications, and as a solubilizer [5, 6]. Currently, it has been expanded to include synthetic ethers, such as those produced by reacting alcoholic glucose solutions with hydrochloric acid, as well as polysaccharides [7-9].

Cardiac glycosides are drugs used to treat certain irregular heartbeats and heart failure [10, 11]. They belong to one of several pharmacological classes that have frequently been developed from foxglove plants, such as Digitalis lanata and Digitalis purpurea, and are used to treat cardiac and associated diseases [12, 13]. The reason foxglove is grown for medicinal purposes are that it produces the cardiac glycoside digoxin. Although this substance is dangerous in large concentrations, it is occasionally used in modest doses to treat heart failure and some types of irregular cardiac rhythms [14, 15]. Digoxin, often known as digitalis, improves the efficiency with which a damaged or frail heart pumps [16, 17]. It increases blood circulation, boosts the force of the heart muscle's contractions, and aids in reestablishing a regular, steady heartbeat [18, 19]. One of the treatments for heart failure symptoms is digoxin, which improves myocardial contractility. This is likely due to the inhibition of sodium-potassium ATPase, which results in intracellular retention of Na^+ and increased intracellular Ca^{2+} concentrations due to the action of the Na^+-Ca^{2+} exchanger [20, 21].

Due to its effectiveness, digoxin must be identified in clinical, pharmaceutical, and dietary samples. Numerous studies have been conducted to enhance the sensing performance using artificial intelligence-assisted electrocardiography [22], immunochromatography [23], fluorescent aptasensors [24], colorimetric aptasensors [25], radioimmunoassay [26], localized surface plasmon resonance-based nanobiosensors [27], high-performance liquid chromatography [28] and electrochemical sensors [29-34]. However, the sensor precision is decreased by the presence of interference organic and inorganic chemical substances in clinical, dietary, and pharmaceutical samples. Electrochemical sensors have shown commendable precision and selectivity for Digoxin determination in actual samples containing the interferants among the sensors. Additionally, these sensors are simple, quick, and affordable [35, 36]. Therefore, additional studies are required to enhance the detecting capabilities of electrochemical sensors. According to studies, nanostructures, composites, and nanohybrids can increase the selectivity and sensitivity of electrochemical sensors [37-39]. As a result, the objective of the current study is to create a nanocomposite of Ag_2S/CNTs by electrodeposition on the GCE surface in order to use it as a sensitive and accurate electrochemical sensor to quantify digoxin in a prepared genuine sample of foxglove.

2. EXPERIMENT

2.1. Synthesis of Ag_2S/CNTs nanocomposite

In a standard three-electrode electrochemical cell with clean GCE as the working electrode, Pt wire as the counter, and Ag/AgCl (3 M KCl) as the reference electrode, the Ag_2S/CNTs nanocomposite was electrodeposited on clean GCE using an electrochemical workstation potentiostat (Xiamen Tob New Energy Technology Co., Ltd., China) [40]. The electrodeposition electrolyte contained an equal volume ratio of 10 mM $AgNO_3$ (≥99.0%, Sigma-Aldrich), 50 mM $Na_2S_2O_3$ (99%, Sigma-Aldrich), and 1 g/l dispersed CNTs (Zhengzhou Yihang Water Purification Materials Co., Ltd., China). The electrodeposition of the Ag_2S/CNTs nanocomposite was conducted at 1 V for 300s at room temperature. For comparison, CNTs modified GCE (CNTs/GCE) was prepared in the same

procedure using a mixture of CNTs and 1 mM HNO_3 (69%, Sigma-Aldrich) equal volume ratio, and Ag_2S modified GCE (Ag_2S/GCE) was electrodeposited in the identical electrodeposition procedure from a mixture of the equal volume ratio of 10 mM $AgNO_3$ and 50 mM $Na_2S_2O_3$.

2.2. Flower sample preparation

Samples of foxglove were gathered in the Chinese region of Yunnan. 100 mL of ethanol was added to 500 g of pureed foxglove. The mixture was sonicated for 12 minutes at 25 °C, at which point it was filtered. The 0.1 M PBS was prepared using the liquid extracts.

2.3. Measurement instruments

The crystalline phase and surface morphology of the nanostructures were studied using X-ray diffraction (XRD) and field-emission scanning electron microscopy (FE-SEM). The three measurements—cyclic voltammetry (CV), differential pulse voltammetry (DPV), and amperometry—were carried out in a standard three-electrode electrochemical cell using the modified and unmodified GCE as the working electrode on an electrochemical workstation potentiostat (Xiamen Tob New Energy Technology Co., Ltd., China). The electrolyte of electrochemical studies was 0.1 M phosphate buffer solution (PBS) with pH 7.4 prepared from 0.1M NaH_2PO_4 (99%, Sigma-Aldrich) and 0.1M Na_2HPO_4 (99%) in a ratio of 1:1 by volume per volume. The digoxin ELISA Kit was also utilized for analysis of Digoxin content in prepared real samples.

3. RESULTS AND DISCUSSION

3.1. Structural analyses

Figure 1 shows the FE-SEM micrographs of the electrodeposited CNTs, Ag_2S, and Ag_2S/CNT nanocomposite on GCE. As can be seen in Figure 1a, the electrodeposited CNTs have formed high-density tubular networks on the GCE surface, with an average diameter of 120nm and a length of several micrometers. The nanostructures can connect to one another and create a structure that resembles a network during the electrodeposition of CNTs. Figure 1b's FE-SEM micrographs of the electrodeposited Ag_2S/CNTs nanocomposite reveal that a dense layer of Ag_2S nanoparticles (30nm in diameter) has grown on the entire surface of the 1D CNTs, forming a hierarchical nanostructure that has a sizable surface area and is very effective at transporting charge carriers along the axial direction [41-43].

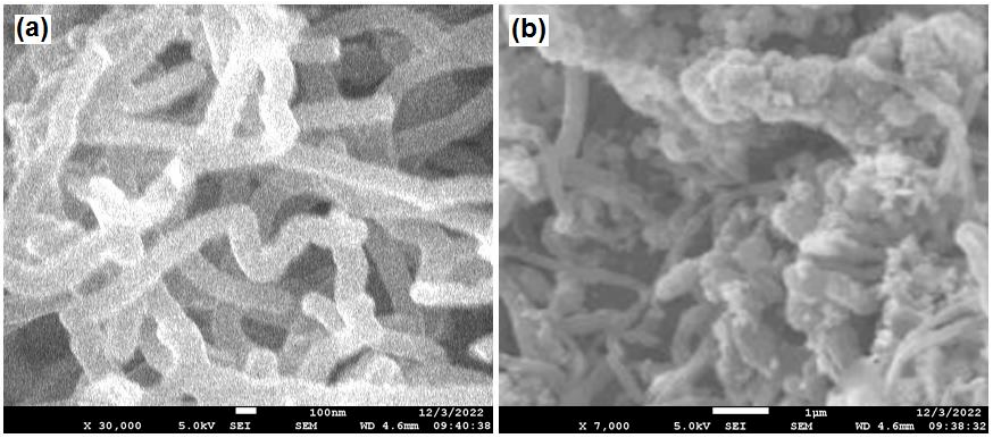

Figure 1. The FE-SEM micrographs of the electrodeposited (a) CNTs, (b) Ag_2S/CNTs nanocomposite on GCE

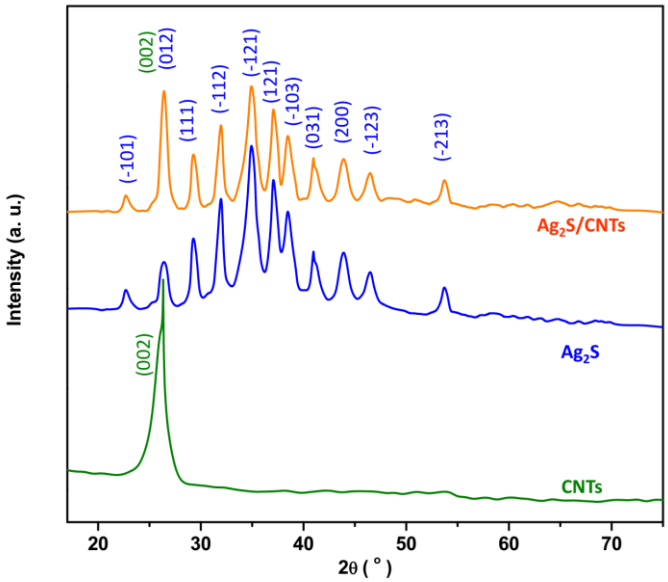

Figure 2. XRD profile of powders of electrodeposited CNTs, Ag_2S and Ag_2S/CNTs nanocomposite.

Figure 2 displays the findings of the structural characterization of powders of electrodeposited CNTs, Ag_2S, and Ag_2S/CNT nanocomposite. The usual crystalline aspect of the CNTs structure was suggested by the XRD profile of CNTs, which exhibits a strong diffraction peak at 26.33° (JCPDS card No. 96-101-1060) [44-46]. According to the XRD profiles of Ag_2S and Ag_2S/CNTs nanocomposite, there are diffraction peaks at 22.69°, 26.34°, 29.24°, 32.01°, 34.96°, 37.03°, 38.54°, 40.96°, 43.85°, 46.48°, and 53.78°, which are indexed to (-101), (012), (111), (-112), (-121), ((JCPDS card No. 14-0072) [47-49]. Additionally, the XRD profile of the Ag_2S/CNTs nanocomposite shows the CNTs' extra diffraction peak (002), indicating that the electrodeposition of the Ag_2S/CNTs nanocomposite's well-crystalline hierarchical nanostructure on the GCE was successful.

3.2. Electrochemical studies

Ag_2S/GCE and Ag_2S/CNTs/CV GCE's responses are shown in Figure 3 for the potential window of 0 V to 60 V with a scanning rate of 30 mV/s in 0.5 M NaOH. The electrochemical behavior of modified Ag_2S electrodes in NaOH electrolyte solution is seen to have two peaks at potentials of 0.33 V and 0.55 V, respectively. This suggests the following reactions [50-52]:

$$Ag_2S + OH^- \Leftrightarrow Ag_2S(OH) + e^-$$
$$Ag_2S \Leftrightarrow 2Ag^+ + S^{2-}$$

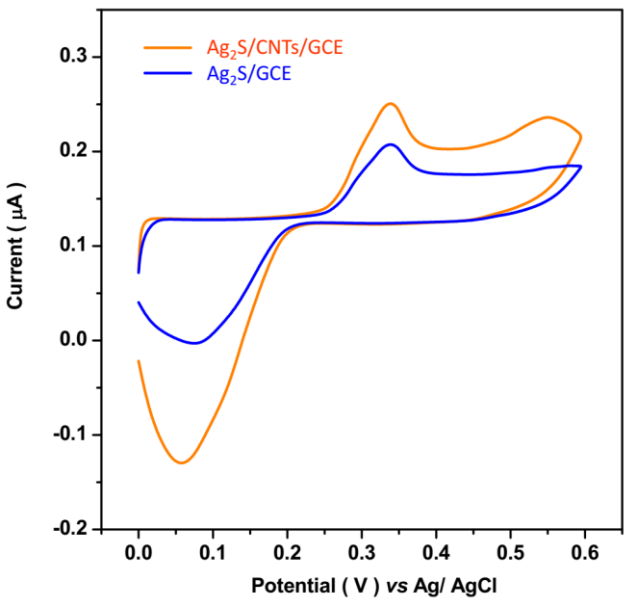

Figure 3. CV response of Ag_2S/GCE and Ag_2S/CNTs/GCE at the potential window from 0.0 V to 0.60 V with a scanning rate of 30 mV/s in 0.5 M NaOH.

In the potential window of 0.40 V to 0.65 V with a scanning rate of 15 mV/s into 0.1M PBS, Figure 4 shows the DPV curves of the bare GCE, CNTs/GCE, Ag2S/GCE, and Ag2S/CNTs/GCE in both the absence and addition of 1 ng/mL Digoxin. As can be seen, when digoxin is absent, none of the electrodes exhibit any distinguishing peak in the DPV curves. While CNTs/GCE, Ag_2S/GCE, and Ag_2S/CNTs/GCE all exhibit anodic peaks at 0.52 V, 0.51 V, and 0.51 V, respectively, which are connected to the oxidation glucose moiety of Digoxin, the DPV curve of bare GCE does not show any noticeable peak after the addition of Digoxin solution [53-55]. The DPV curves demonstrate that the peak current of Ag_2S/CNTs/GCE is remarkable for its great peak current at a lower potential of 0.51 V, which is nearly 2-fold, and 2.6-fold higher than the peak currents of CNTs/GCE and Ag_2S/GCE, respectively. It is found that Ag_2S nanoparticles can reduce the oxidation potential [56], and CNTs with large specific surface area and abundant functional groups can provide a good conductive platform for electrocatalysis reactions in electrochemical systems [57]. The Ag_2S catalyst has been completely encircled by the CNTs, as seen by FE-SEM micrographs of the Ag_2S/CNT nanocomposite (Figure 1c), and complex tubular morphologies of hierarchical nanostructures have been created. Fast

access to active areas is made possible by the hierarchically porous nanostructure of nanocomposite, which also ensures a durable composite structure [58-60]. The high dispersion of Ag_2S nanoparticles, which might offer a significant effective surface area for the transport of ions, is likely a contributing factor to the increased electrocatalytic activity of Ag_2S/CNTs. Additionally, the high conductivity of CNTs can help in electron and mass transmission [61-63]. In the subsequent electrochemical sensing of digoxin, only Ag_2S/CNTs/GCE was used due to the synergistic effects of Ag_2S and CNTs in catalytic processes for the determination of digoxin.

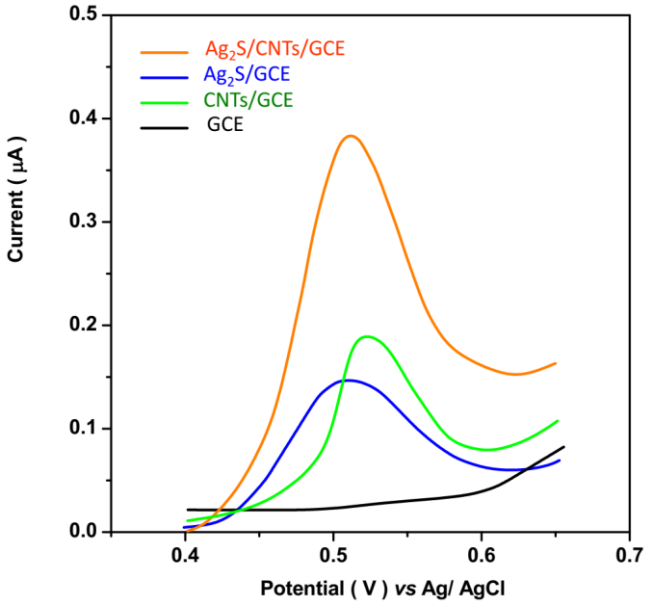

Figure 4. DPV curves of the bare GCE, CNTs/GCE, Ag_2S/GCE and Ag_2S/CNTs/GCE in the potential window of 0.40 V to 0.65 V with a scanning rate of 15 mV/s into 0.1M PBS in both the absence and addition of 1 ng/mL Digoxin.

The calibration plot of Ag_2S/CNTs/GCE under the sequential injection of 1 ng/mL Digoxin solution into 0.1 M PBS (pH 7.4) at potential of 0.51 V is shown in Figure 5 along with the results of the amperometry analyses. Ag_2S/CNTs/GCE responds quickly to the addition of digoxin, exhibits a stable amperometric response, and exhibits a linear relationship with the digoxin concentration from 0 to 24ng/mL. The findings show that the Ag_2S/CNTs/GCE can effectively transfer electrons and collect Digoxin molecules from the electrolyte [64, 65]. The sensitivity is 0.31287μA/ng.mL^{-1}, the detection limit is 0.001ng/mL, and the signal-to-noise ratio is 3. The analytical figures of merit for the determination of digoxin in this investigation when compared with recently reported digoxin sensors are summarized in Table 1. It has been noted that the produced digoxin sensor's linear range and detection limit in this work have been improved and are on par with or better than those reported in more recent publications. The synergy between 1D porous nanostructures, ultra-small Ag_2S nanocrystals localized on CNTs surface, and more active sites may be responsible for the hierarchical hybrid nanostructured Ag_2S/CNTs' improved performance [58, 66].

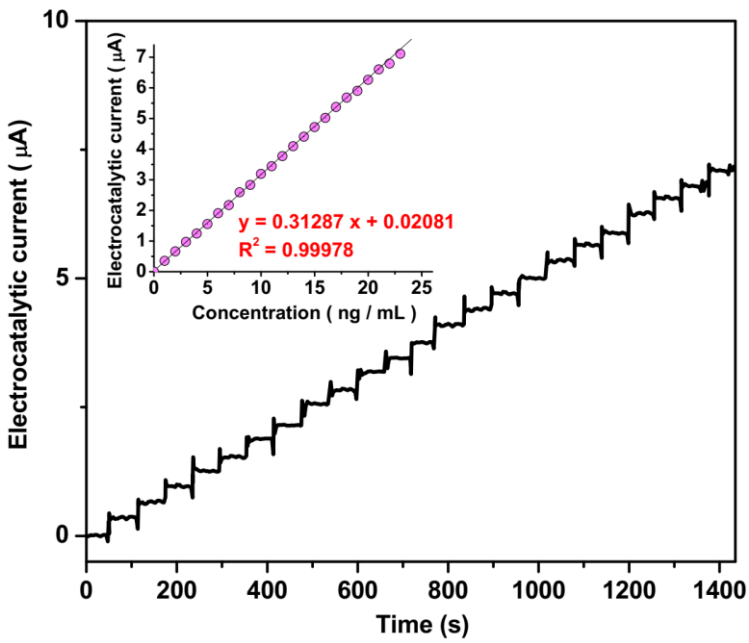

Figure 5. The results of amperometry analyses and corresponded calibration plot of Ag_2S/CNTs/GCE under consecutive injection 1 ng/mL Digoxin solution into 0.1 M PBS (pH 7.4) at potential of 0.51 V.

Table 1. The analytical figures of merit for determination of Digoxin in this study compared with recent reported Digoxin sensors.

Electrode	Technique	LOD (ng/mL)	Linear range (ng/mL)	Ref.
Ag_2S/CNTs/GCE	Amperomertry	0.001	0 to 24	This study
Enzyme immobilized Carbon paste electrode	Enzyme Immunoassay	5×10^{-2}	---	[29]
Au NPs/GO composites	LSV	0.19	0.1 to 2	[30]
Ag NPs/GO	DPV	0.234×10^{-3}	780×10^{-3} to 0.780	[31]
Au NPs/FTO	DPV	0.01	0.02 to 0.2	[32]
50-base DNA oligonucleotide/Au electrode	SWV	0.5	0.5 to 2.0	[33]
Au NPS suspension	Fluorescence	0.260	0 to 23.427	[34]

LSV: Linear sweep voltammetry; SWV: Square wave voltammetry

The interferences of a few substances that are present in flower extract were studded using amperomertic analysis via Ag_2S/CNTs/GCE at a potential of 0.51 V in 0.1M PBS under the addition of 1 ng/mL Digoxin and 10 ng/mL of interfering species in order to evaluate the interference effect on the determination of Digoxin in the flower sample. The interfering species are reported in Table 2, which shows that there is no obvious change in the Digoxin electrocatalytic current after the addition of

interfering species. It follows that the proposed Digoxin sensor shows excellent selectivity for Digoxin determination in floral extract.

Table 2. Results of electrocatalytic currents of Ag_2S/CNTs/GCE using amperomertic analysis at 0.51 V into 0.1M PBS in addition 2 ng/mL Digoxin and 10 ng/mL of interfering species.

Specie	**Added (ng/mL)**	**Electrocatalytic signal (µA)**	**RSD**
Digoxin	1	0.3131	±0.0097
Quercetin	10	0.0632	±0.0029
Rutin	10	0.0711	±0.0028
Fisetin	10	0.0523	±0.0034
Myricetin	10	0.0380	±0.0022
Morin	10	0.0253	±0.0019
Vanillic acid	10	0.0632	±0.0024
ρ-hydroxybenzoic acid	10	0.0700	±0.0024

For the purpose of determining Digoxin in prepared genuine samples from foxglove flowers, the accuracy of Ag_2S/CNTs/GCE were evaluated (S1 to S4). Table 3 displays the outcomes of amperometric studies at 0.51 V using the Digoxin ELISA kit for determining Digoxin in prepared real samples both before and after Digoxin administration. A manufactured genuine sample (S1digoxin)'s content was determined using amperometric measurements, along with the associated calibration plot of Ag_2S/CNTs/GCE, in Figure 6. The calibration curve reveals that the prepared real sample's digoxin content is 0.215 ng/mL, which is similar to the amount of digoxin discovered by the ELISA kit (0.212 ng/mL) displayed in Table 3. Table 3 shows that there is good agreement between the findings of the two studies for other samples (S2 to S4). Additionally, Table 3's results from analytical experiments utilizing the standard addition procedure demonstrate acceptable RSD values (3.47% to 4.41%). These results demonstrate that the suggested approach has been effectively used to determine digoxin in floral extract.

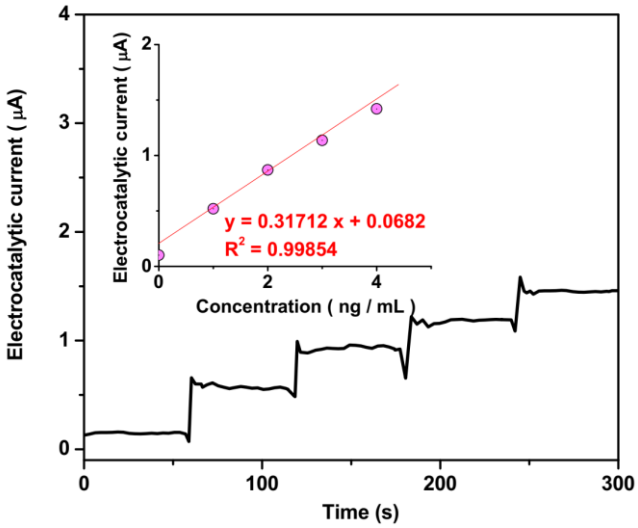

Figure 6. Amperometric analyses and the corresponding calibration plot of Ag_2S/CNTs/GCE for addition of Digoxin solution (0 to 4 ng/mL) into0.1 M PBS prepared with real sample from foxglove flower (S1) at 0.51 V.

Table 3. The results of amperometric analyses at 0.51 V and Digoxin ELISA kit for determination Digoxin in prepared real samples before and after addition Digoxin.

Content of Digoxin **in prepared samples (ng/mL)**				
Sample No.	**Amperometry**		**Digoxin ELISA Kit**	
	Ag_2S/CNTs/GCE	**RSD (%)**	**ELISA**	**RSD (%)**
S1	0.215	±3.47	0.212	±4.10
S2	0.189	±4.21	0.193	±4.25
S3	0.194	±4.41	0.199	±4.21
S4	0.205	±4.05	0.202	±3.98

4. CONCULUSION

The current study concentrated on creating an Ag_2S/CNT nanocomposite by electrodepositing it on the surface of a GCE as a sensitive and precise electrochemical sensor to assess the amount of digoxin in a manufactured genuine sample of foxglove. The results of the structural analyses demonstrated that the electrodeposited Ag_2S/CNTs nanocomposite contained numerous Ag_2S nanoparticles that densely grew on the entire surface of the 1D CNTs. This nanocomposite also formed a well-crystalline hierarchical nanostructure that allowed it to transport charge carriers very well along the axial direction and possessed a sizable surface area. As a sensitive and selective Digoxin sensor, Ag_2S/CNTs/GCE demonstrated a quick reaction time, a steady electrocatalytic response, and a linear relationship to the concentration of Digoxin from 0 to 24ng/mL, according to the electrochemical results. The sensitivity was 0.31287μA/ng.mL^{-1}, and the detection limit was 0.001ng/mL. The accuracy of Ag2S/CNTs/GCE was tested for the purpose of determining Digoxin in genuine samples of

foxglove flowers that had been prepared. The findings indicated acceptable RSD values and showed good agreement between the conclusions of the two studies for further samples. These results showed that the suggested procedure has been successfully used to determine digoxin in floral extract.

References

1. C.G. Awuchi, *Journal of Food and Pharmaceutical Sciences*, 7 (2019) 131.
2. L. Sun, G. Wang, C. Zhang, Q. Jin and Y. Song, *Nanotechnology Reviews*, 10 (2021) 1339.
3. W. Zhang, S. Wang, J. Yang, C. Kang, L. Huang and L. Guo, *Environmental and Experimental Botany*, 194 (2022) 104703.
4. M. Yang, C. Li, Y. Zhang, D. Jia, X. Zhang, Y. Hou, R. Li and J. Wang, *International Journal of Machine Tools and Manufacture*, 122 (2017) 55.
5. Y. Yang, M. Xu, Z. Wan and X. Yang, *Current Opinion in Food Science*, 43 (2022) 91.
6. T. Gao, C. Li, Y. Zhang, M. Yang, D. Jia, T. Jin, Y. Hou and R. Li, *Tribology International*, 131 (2019) 51.
7. J. Ran, H. Sun, Y. Xu, T. Wang and R. Zhao, *International Journal of Food Properties*, 19 (2016) 2396.
8. G. Luo, J. Xie, J. Liu, Q. Zhang, Y. Luo, M. Li, W. Zhou, K. Chen, Z. Li and P. Yang, *Chemical Engineering Journal*, 451 (2022) 138549.
9. J. Rouhi, S. Kakooei, M.C. Ismail, R. Karimzadeh and M.R. Mahmood, *International Journal of Electrochemical Science*, 12 (2017) 9933.
10. K. Georgiev, N. Hvarchanova, M. Georgieva and B. Kanazirev, *International Journal of Pharmaceutical Research*, 11 (2019) 524.
11. C. Zhao, M. Xi, J. Huo and C. He, *Physical Chemistry Chemical Physics*, 23 (2021) 23219.
12. U. Bavendiek, D. Berliner, L.A. Davila, J. Schwab, L. Maier, S.A. Philipp, A. Rieth, R. Westenfeld, C. Piorkowski and K. Weber, *European journal of heart failure*, 21 (2019) 676.
13. S. Guo, C. Li, Y. Zhang, Y. Wang, B. Li, M. Yang, X. Zhang and G. Liu, *Journal of Cleaner Production*, 140 (2017) 1060.
14. Y. Wang, C. Li, Y. Zhang, M. Yang, B. Li, L. Dong and J. Wang, *International Journal of Precision Engineering and Manufacturing-Green Technology*, 5 (2018) 327.
15. H. Maleh, M. Alizadeh, F. Karimi, M. Baghayeri, L. Fu, J. Rouhi, C. Karaman, O. Karaman and R. Boukherroub, *Chemosphere*, (2021) 132928.
16. Y. Wang, Q. Ma, S. Zhang, H. Liu, B. Zhao, B. Du, W. Wang, P. Lin, Z. Zhang and Y. Zhong, *Frontiers in pharmacology*, 11 (2020) 186.
17. M. Yang, C. Li, Y. Zhang, D. Jia, R. Li, Y. Hou, H. Cao and J. Wang, *Ceramics International*, 45 (2019) 14908.
18. T.A. Quinn and P. Kohl, *Physiological reviews*, 101 (2021) 37.
19. Y. Yang, Y. Wang, C. Zheng, H. Lin, R. Xu, H. Zhu, L. Bao and X. Xu, *Chemical Engineering Journal*, 430 (2022) 133166.
20. J.T. Bigger Jr, *The Journal of Clinical Pharmacology*, 25 (1985) 514.
21. J. Zhang, C. Li, Y. Zhang, M. Yang, D. Jia, G. Liu, Y. Hou, R. Li, N. Zhang and Q. Wu, *Journal of cleaner production*, 193 (2018) 236.
22. D.-W. Chang, C.-S. Lin, T.-P. Tsao, C.-C. Lee, J.-T. Chen, C.-S. Tsai, W.-S. Lin and C. Lin, *International journal of environmental research and public health*, 18 (2021) 3839.
23. K. Omidfar, S. Kia, S. Kashanian, M. Paknejad, A. Besharatie, S. Kashanian and B. Larijani, *Applied biochemistry and biotechnology*, 160 (2010) 843.
24. A.S. Emrani, S.M. Taghdisi, N.M. Danesh, S.H. Jalalian, M. Ramezani and K. Abnous, *Analytical Methods*, 7 (2015) 3814.

25. A.S. Emrani, N.M. Danesh, P. Lavaee, S.H. Jalalian, M. Ramezani, K. Abnous and S.M. Taghdisi, *Analytical Methods*, 7 (2015) 3419.
26. G.C. Oliver, B.M. Parker and C.W. Parker, *The American journal of medicine*, 51 (1971) 186.
27. A. Nikfarjam, A.H. Rezayan, G. Mohammadkhani and J. Mohammadnejad, *Plasmonics*, 12 (2017) 157.
28. K.L. Kelly, B.A. Kimball and J.J. Johnston, *Journal of Chromatography A*, 711 (1995) 289.
29. K.R. Wehmeyer, H.B. Halsall, W.R. Heineman, C.P. Volle and I.W. Chen, *Analytical Chemistry*, 58 (1986) 135.
30. S. Kaleem, S. Mehmood, M. Chaudhry, A. Ali, M.F. Bhopal and A.S. Bhatti, *Sensors and Actuators A: Physical*, 318 (2021) 112489.
31. M.H. Mashhadizadeh, N. Naseri and M.A. Mehrgardi, *Analytical Methods*, 8 (2016) 7247.
32. H. Bagheri, R. Talemi and A. Afkhami, *Rsc Advances*, 5 (2015) 58491.
33. M.S. Wijesinghe, W. Ngwa and K.F. Chow, *ChemistrySelect*, 5 (2020) 2408.
34. A. Sarreshtehdar Emrani, N.M. Danesh, P. Lavaee, S.H. Jalalian, M. Ramezani, K. Abnous and S.M. Taghdisi, *Analytical Methods*, 7 (2015) 3419.
35. L. Tang, Y. Zhang, C. Li, Z. Zhou, X. Nie, Y. Chen, H. Cao, B. Liu, N. Zhang and Z. Said, *Chinese Journal of Mechanical Engineering*, 35 (2022) 1.
36. H. Karimi-Maleh, R. Darabi, M. Shabani-Nooshabadi, M. Baghayeri, F. Karimi, J. Rouhi, M. Alizadeh, O. Karaman, Y. Vasseghian and C. Karaman, *Food and Chemical Toxicology*, 162 (2022) 112907.
37. M.R. Ganjali, F.G. Nejad, H. Beitollahi, S. Jahani, M. Rezapour and B. Larijani, *International Journal of Electrochemical Science* 12 (2017) 3231.
38. S.B. Khan, M.M. Rahman, K. Akhtar, A.M. Asiri, K.A. Alamry, J. Seo and H. Han, *International Journal of Electrochemical Science*, 7 (2012) 10965.
39. L. Shi, Y. Huang, N. Wu, Z. Wang and J. Tan, *International Journal of Electrochemical Science*, 16 (2021) 21048.
40. X.Y. Guo, S.Y. Cheng, P.M. Lu and H.F. Zhou. *Preparation of Ag2S thin films by electro-deposition*. in *Materials Science Forum*. 2011: Trans Tech Publ.
41. J. Xiong, C. Han, W. Li, Q. Sun, J. Chen, S. Chou, Z. Li and S. Dou, *CrystEngComm*, 18 (2016) 930.
42. H. Savaloni, E. Khani, R. Savari, F. Chahshouri and F. Placido, *Applied Physics A*, 127 (2021) 1.
43. H. Karimi-Maleh, C. Karaman, O. Karaman, F. Karimi, Y. Vasseghian, L. Fu, M. Baghayeri, J. Rouhi, P. Senthil Kumar and P.-L. Show, *Journal of Nanostructure in Chemistry*, (2022) 1.
44. H. Soleimani, N. Yahya, M. Baig, L. Khodapanah, M. Sabet, M. Burda, A. Oechsner and M. Awang, *Oil Gas Res*, 1 (2015) 1000104.
45. R. Savari, J. Rouhi, O. Fakhar, S. Kakooei, D. Pourzadeh, O. Jahanbakhsh and S. Shojaei, *Ceramics International*, 47 (2021) 31927.
46. H. Karimi-Maleh, H. Beitollahi, P.S. Kumar, S. Tajik, P.M. Jahani, F. Karimi, C. Karaman, Y. Vasseghian, M. Baghayeri and J. Rouhi, *Food and Chemical Toxicology*, (2022) 112961.
47. G. Wang, J. Liu, L. Zhu, Y. Guo and L. Yang, *RSC advances*, 9 (2019) 29936.
48. Y. Yang, H. Zhu, X. Xu, L. Bao, Y. Wang, H. Lin and C. Zheng, *Microporous and Mesoporous Materials*, 324 (2021) 111289.
49. Y. Zhang, H.N. Li, C. Li, C. Huang, H.M. Ali, X. Xu, C. Mao, W. Ding, X. Cui and M. Yang, *Friction*, 10 (2022) 803.
50. A. Arulraj, N. Ilayaraja, V. Rajeshkumar and M. Ramesh, *Scientific Reports*, 9 (2019) 10108
51. C. Horwood and M. Stadermann, *Electrochemistry Communications*, 88 (2018) 105.
52. X. Wang, C. Li, Y. Zhang, H.M. Ali, S. Sharma, R. Li, M. Yang, Z. Said and X. Liu, *Tribology International*, 174 (2022) 107766.

53. N. Butwong, T. Kunawong and J.H.T. Luong, *Nanomaterials*, 10 (2020) 1583.
54. M.-R. Wang, L. Deng, G.-C. Liu, L. Wen, J.-G. Wang, K.-B. Huang, H.-T. Tang and Y.-M. Pan, *Organic letters*, 21 (2019) 4929.
55. C. Xin, L. Changhe, D. Wenfeng, C. Yun, M. Cong, X. Xuefeng, L. Bo, W. Dazhong, H.N. Li and Y. Zhang, *Chinese Journal of Aeronautics*, (2021) 1.
56. C.-Y. Li, Y.-J. Cai, C.-H. Yang, C.-H. Wu, Y. Wei, T.-C. Wen, T.-L. Wang, Y.-T. Shieh, W.-C. Lin and W.-J. Chen, *Electrochimica acta*, 56 (2011) 1955.
57. W.-D. Zhang, B. Xu and L.-C. Jiang, *Journal of Materials Chemistry*, 20 (2010) 6383.
58. H. Han, Z. Bai, T. Zhang, X. Wang, X. Yang, X. Ma, Y. Zhang, L. Yang and J. Lu, *Nano energy*, 56 (2019) 724.
59. Z. Savari, S. Soltanian, A. Noorbakhsh, A. Salimi, M. Najafi and P. Servati, *Sensors and Actuators B: Chemical*, 176 (2013) 335.
60. M. Liu, C. Li, Y. Zhang, Q. An, M. Yang, T. Gao, C. Mao, B. Liu, H. Cao and X. Xu, *Frontiers of Mechanical Engineering*, 16 (2021) 649.
61. S. Xie, X.-L. Tong, G.-Q. Jin, Y. Qin and X.-Y. Guo, *Journal of Materials Chemistry A*, 1 (2013) 2104.
62. R. Savari, H. Savaloni, S. Abbasi and F. Placido, *Sensors and Actuators B: Chemical*, 266 (2018) 620.
63. H. Savaloni, R. Savari and S. Abbasi, *Current Applied Physics*, 18 (2018) 869.
64. X. Wu, C. Li, Z. Zhou, X. Nie, Y. Chen, Y. Zhang, H. Cao, B. Liu, N. Zhang and Z. Said, *The International Journal of Advanced Manufacturing Technology*, 117 (2021) 2565.
65. X. Cui, C. Li, Y. Zhang, Z. Said, S. Debnath, S. Sharma, H.M. Ali, M. Yang, T. Gao and R. Li, *Journal of Manufacturing Processes*, 80 (2022) 273.
66. B. Li, C. Li, Y. Zhang, Y. Wang, D. Jia and M. Yang, *Chinese Journal of Aeronautics*, 29 (2016) 1084.